Proposal of Switched-mode Matching Circuit in Power Supply for Wireless Power Transfer Using Magnetic Resonance Coupling

Keisuke Kusaka
Dept. of Electrical, Electronics and Information Engineering
Nagaoka University of Technology
Nagaoka Niigata, Japan
kusaka@stn.nagoakaut.ac.jp

Jun-ichi Itoh
Dept. of Electrical, Electronics and Information Engineering
Nagaoka University of Technology
Nagaoka Niigata, Japan
itoh@vos.nagaokaut.ac.jp

***Abstract*— This paper discusses on the matching circuit in the power supply for wireless power transfer using a magnetic resonance coupling (MRC). The MRC is desired to operate at high frequency in the Industry Science Medical (ISM) bands such as 13.56 MHz. The resonance with high quality factor between the transmitting side and receiving side enables high efficiency for wireless power transfer. Therefore, the output frequency of the inverter must be aligned identically to the resonance frequency of the resonance coils in purpose of keeping the high transmission efficiency. In addition, the output impedance of the power supply has to be matched to the characteristic impedance of the transmission line that is despites to the output frequency. In this paper, the Switched-mode Matching Circuit (SMC) which operates to stabilize the output impedance of the inverter is proposed by the authors. The results confirmed in experimental and simulation demonstrates that, the SMC able to provide the variation of the output impedance.**

I. INTRODUCTION

In recent years, the wireless power transfer systems are increasingly studied [1-2]. Especially, the wireless power transfer using a magnetic resonant coupling (MRC) which is reported in 2007 has been attracted in community [3-5]. The MRC shows advantages compared to other wireless power transfer methods such as an electromagnetic induction and microwave power transfer. First, the MRC enables a wireless power transfer at middle range distance such as 1 m at high efficiency over 90%. Second, the declination in transmission efficiency caused by position gap is relatively small. The MRC is found suitable to apply in the battery chargers for electric vehicle (EV). The transmitting device and the receiving device are placed on the ground of parking areas, and underneath of the EV respectively. The batteries are charged automatically when the EV is parked at the parking areas. The wireless power transfer system enables to improve the conveniences of the users.

The studies about the resonance coils and a rectifier in the receiving side have been discussed actively [6-8]. However, a research about high frequency power supply and matching circuit are not discussed. In the MRC system, the wire length of the resonance coil decreases commensurately with increasing transmission frequency. The resonance coils must be mounted on the EV. Furthermore, the resonance coils are required being small size and light weight. The wireless power transfer using a MRC satisfies to the standard of Industry Science Medical (ISM) band of around 13.56 MHz. Therefore, a high frequency inverter achieves high efficiency is needed.

In addition, a reflected power occurs at the boundary point of the impedance in high frequency region. In order to suppress the reflected power between the power supply and transmission line, a matching circuit which consists of the inductor and capacitor is placed at the output terminal of the inverter. Generally, the high frequency inverters, which are used in the high frequency applications such as a plasma generation, often operated in a constant output frequency. Thus, the matching circuit needs unique parameters to consistent the output impedance with the characteristic impedance of the transmission line. However, the resonance frequency of the resonance coils is fluctuated according to the transmission distance in the wireless power transfer systems. Therefore, the output frequency of the inverter must be aligned identically to the resonance frequency of the resonance coils in order to keep the high transmission efficiency. In a conventional matching circuit, the matching circuit has a meter movement because the matching circuit consists of the inductor, variable capacitors and stepping motors. Therefore, the meter movements decrease a lifetime and response speed of the matching circuit.

Firstly, the characteristics of the wireless power transfer system with MRC and fundamental characteristics of the

reflected power are described. The reflected power occurs due to the impedance mismatch. Secondary, the output impedance of the inverter is discussed in this paper. A proposed circuit is designed base on the matching circuit with Low-frequency Pass Filter (LPF) type. Finally, the Switched-mode Matching Circuit (SMC), which enable to adjust the output impedance of the inverter using the MOSFETs. The SMC can improve the lifetime and response speed of the matching circuit. The experimental verification of the SMC is demonstrated.

II. WIRELESS POWER TRANSFER SYSTEM

Fig. 1 illustrates the system configuration of a wireless power transfer system using the MRC. The system consists of the function generator (FG), the radio frequency (RF) power supply matched to 50 Ω, two resonance coils and the load. Signal from the FG are amplified by RF power supply. The RF power supply which can control the output travelling power is composed by an A-class linear amplifier in the test bench. The amplified power is supplied to the resonance coils. The resonance coils are designed according to the specification shown in Table I. The resonance coil which placed in the transmitting side is called as the transmitting coil. Also the resonance coil, which placed in the receiving side, is known as the receiving coil. Besides the resonance coils have a same structure of the helical antenna. Thus, the resonance coils have a feeding point at the center of the resonance coil. In consequence, the resonance coils have a self-resonance frequency f_0 due to distributed capacitance C of winding pitch and winding inductance L. The self-resonance frequency is obtained by $f_0=1/\{2\pi(LC)^{0.5}\}$.

Fig. 2 presents the equivalent circuit of the wireless power transfer using the MRC [9]. The equivalent circuit of the one-sided resonance coil is presented as a series connected RLC circuit. Thus, the MRC has a same equivalent circuit to the magnetic induction which has series resonance capacitors in both sides; transmitting and receiving, to have a resonance. Equation (1) presents the transmitting efficiency, where $S_{21}(\omega)$ is the transmission coefficient which is obtained by (2) [10], L_m is the mutual inductance, R is the simulated resistance of the radiation loss, copper loss of the resonance coils and dielectric loss which occurs in the braces for the resonance coils, Z_0 is the characteristic impedance of the transmission line, and ω is the transmission angular frequency.

$$\eta(\omega)=\left|S_{21}(\omega)\right|^2\times 100 \tag{1}$$

$$S_{21}(\omega)=2jL_mZ_0\omega\Big/\left[L_m^2\omega^2-\left\{R+\left(\omega L-\frac{1}{\omega C}\right)\right\}^2+2jZ_0\left\{R+\left(\omega L-\frac{1}{\omega C}\right)\right\}+Z_0^2\right] \tag{2}$$

The transmission coefficient is a proportion of the transmission power to the travelling power. By substituting the resonance angular frequencies ω_m and ω_e into the equation, (3) is obtained

$$S_{21}(\omega_m)=\frac{2}{2-j\dfrac{1}{kQ}},\ S_{21}(\omega_e)=\frac{2}{2+j\dfrac{1}{kQ}} \tag{3}$$

When the transmission frequency equals to the resonance frequencies of ω_m and ω_e, the transmission coefficient $S_{21}(\omega)$ has local maximum value. Note that the ω_e is larger than the ω_m. An electromagnetic field distribution between the transmitting coil and the receiving coil for the wireless power transfer is difference in terms of the resonance frequencies. Furthermore, equation (3) indicates that the product of inductive coupling coefficient k and quality factor Q will affect the transmission efficiency. The inductive coupling decreases in inverse proportion to cube transmission distance. However, the $k\cdot Q$ still remains high because high quality factor Q is in a middle-range distance. Generally, the magnetic induction is operated with low quality factor such as several dozens. On the other hand, the MRC is operated in a few hundred of quality factor.

High quality factor enables high efficiency wireless power transfer. However, the resonance frequency depends on the transmitting distances because of the variation of coupling coefficient k. Therefore, the transmission frequency needs to track to the resonance frequency of the transmitting coils in order to maintain the transmission efficiency.

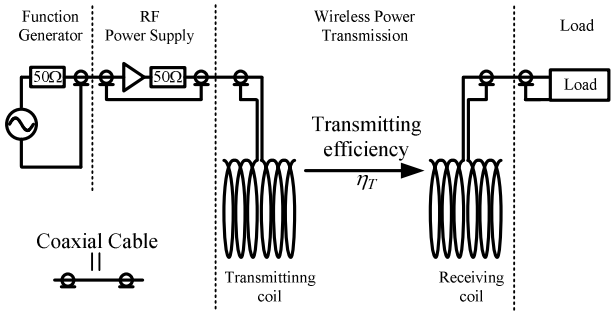

Figure 1. System configuration of wireles power transfer using MRC.

TABLE I. SPECIFICATIONS OF RESONANCE COILS.

Number of turn	6 [turn]
Material	Magnet wire φ2.3[mm]
Radius	20 [cm]
Vertical Height	9.9 [cm]

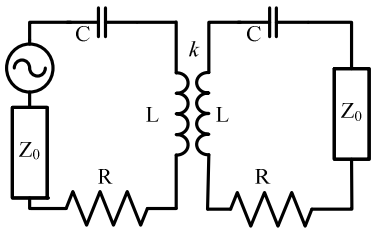

(a) Equivalent circuit.

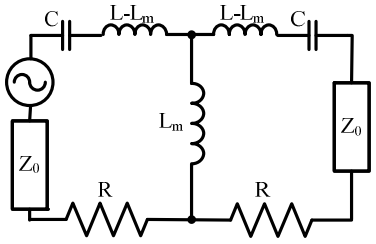

(b) Equivalent circuit of type-T.

Figure 2. Equivalent circuit of the wireless power transfer using a MRC.

III. Fundamental Characteristics of the Reflected Power

Fig. 3 shows the experimental circuit which clarifies the relationship between the travelling power and the reflected power. In Fig. 3, P_F is the travelling power, P_R is the reflected power and P_{Load} is the transmitted power which equals to the consumed power at the load resistance respectively. The resistance load is connected to the RF power supply through the coaxial cable which has characteristic impedance of 50 Ω. In the high frequency region, the reflected power occurs at a certain boundary point of the impedance when the impedance is mismatched.

Fig. 4 shows the characteristics of the reflected power and transmitted power when the travelling power is 100 W in the circuit drawn in Fig. 3. The reflected and transmitted powers depend on the load resistance when the characteristic impedance has a constant value. The consumed power is decreased with increasing the reflected power due to impedance mismatch. The theoretical formulas of the reflected power and transmitted power are obtained by (4) and (5) respectively.

$$P_{Load}^{*} = P_F\left(1-\Gamma^2\right) \tag{4}$$

$$P_R^{*} = P_F\Gamma^2 \tag{5}$$

where Γ is the reflection coefficient which is expressed by

$$\Gamma = \left|\frac{\dot{Z}_0 - \dot{Z}_{Load}}{\dot{Z}_0 + \dot{Z}_{Load}}\right| \tag{6}.$$

The reflection coefficient Γ is decided by using the characteristic impedance of the transmission line $\dot{Z}_0$ and impedance of the load $\dot{Z}_{Load}$. The reflection coefficient Γ indicates the proportion of the reflection voltage to the travelling voltage. Moreover the reflection coefficient Γ follows the proportion of the reflection current to the travelling current. Hence, the ratio of the travelling power to reflected power is a squared reflection coefficient Γ^2. Furthermore, the transmitted power is obtained by subtracting the reflected power from the travelling power. When the characteristic impedance of the transmission line equals to the impedance of the load, reflection coefficient is zero. So, the reflected power does not occur.

The experimental results confirmed that the reflected power which is not consumed at the load has to be suppressed.

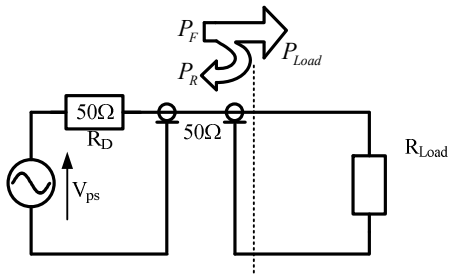

Figure 3. Experimental circuit which clarifies the relationship among a travelling, a reflected and transmitted power.

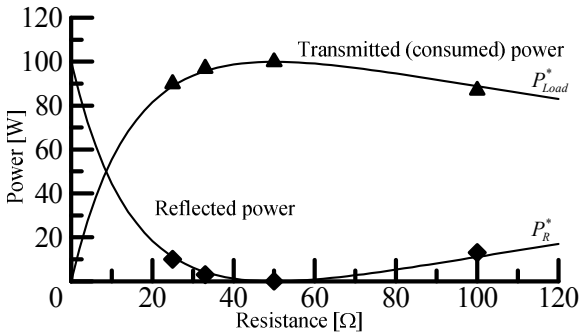

Figure 4. Characteristics of the reflected and transmitted power.

IV. Derivation of Output Impedance of Inverter

Fig. 5 provides an example of the high frequency power supply configuration for a wireless power transmission, where the MRC is used to considerate the output impedance of the inverter. The output impedance of the inverter which is operated in a constant frequency at high frequency with square wave operation is discussed. Note that the inverter does not have a voltage controller. Besides, the matching circuit, which has same circuit configuration to the LPF, is connected to the output terminal of the inverter. Since the LPF circuit consists of an inductor L_m and a capacitor C_m as a matching circuit at one frequency which is used in the design of LPF, the impedance mismatch occurs when the output

frequency is not equals to design frequency. Therefore, the transmission frequency which equals to the output frequency of the inverter has to tracks to the resonance frequency.

Fig. 6 shows the block diagram of the power supply including the matching circuit where E_d is the DC voltage of the inverter, V_{cmd} is the output voltage command for inverter and r_d is the simulated resistance of the voltage drop due to dead time of the inverter. Thus r_d is connected to the matching circuit in series to the inductor in Fig. 5. In this scheme, the output current from the matching circuit is considered as a disturbance. The block diagram clarifies that the output voltage V_{out} is obtained by

$$V_{out} = G_{cmd}(s)V_{cmd} + G_d(s)I_{out} \tag{7}$$

where $G_{cmd}(s)$ is the transfer function in term of output voltage command V_{cmd} and G_d is the disturbance transfer function in term of output current I_{out}. Note that the output impedance is defined as $Z_{out}=\Delta V_{out}/I_{out}$. Therefore, the output impedance of the inverter without an automatic voltage regulator (AVR) is obtained from $\dot{Z}_o=G_d(s)|_{s=j\omega}$ [11]. The output impedance is decided by the disturbance transfer function where $G_d(s)$ is presented by

$$G_d(s) = \frac{\omega_c^2(Ls + r_d)}{s^2 + \frac{r_d}{L}s + \omega_c^2} \tag{8}.$$

By substituting (8) into the equation, the output impedance of the inverter is expressed by (9) where ω_c is the cut-off frequency of the LPF.

$$\dot{Z}_o = G_d(s)|_{s=j\omega} = \frac{r_d\omega_c^4 + j\omega\omega_c^2\left\{L\left(\omega_c^2 - \omega^2\right) - \frac{r_d^2}{L}\right\}}{\left(\omega_c^2 - \omega^2\right)^2 + \left(\frac{r_d}{L}\omega\right)^2} \tag{9}$$

The output frequency of the inverter should be matched to the characteristic impedance of $\dot{Z}_0=\mathrm{Re}[\dot{Z}_0]+j0\ \Omega$. It should be noted that the characteristic impedance does not compose of the imaginary part because the standard of the transmission line does not have characteristic impedance with imaginary part. By solving the simultaneous equation in terms of L and ω_c, the inductance and capacitance of the LPF is obtained by (10) and (11) [12].

$$L_m = \sqrt{\frac{r_d^2\omega^2\,\mathrm{Re}[\dot{Z}_o]}{r_d\omega_c^4 - \left(\omega_c^2 - \omega^2\right)^2\,\mathrm{Re}[\dot{Z}_0]}} \tag{10}$$

$$C_m = \frac{\mathrm{Re}[\dot{Z}_O] - r_d}{\omega^2 L_m\,\mathrm{Re}[\dot{Z}_O]} \tag{11}$$

Where the cut-off frequency is expressed by

$$\omega_c = \omega\sqrt{\frac{\mathrm{Re}[\dot{Z}_o]}{\mathrm{Re}[\dot{Z}_o] - r_d}} = \frac{1}{\sqrt{L_m C_m}} \tag{12}.$$

Therefore, to match the output impedance of the inverter to the characteristic impedance of the transmission line, both the inductance and capacitance should be adjusted. Note that the output voltage of the inverter including the LPF is a sinusoidal waveform due to the resonance when the output impedance is matched.

Fig. 7 presents the frequency characteristic of the output impedance of the inverter which is designed to match the impedance to $50+j0\ \Omega$ at 13.56 MHz where the inductance L_m is 115 nH and the capacitance C_m is 1.15 nF. Fig. 7 shows the design of the output impedance is correct, although both of the output impedance; real part and imaginary parts have variation when the frequency does not equal to the design frequency of the LPF. The reflected power occurs due to the fluctuation of the output impedance between the power supply and transmission line according to (5). Assuming that the frequency fluctuation of the MRC is plus or minus 1 MHz, the output impedance has maximum variation of 30 Ω.

Fig. 8 shows the proportion of the reflected power to the travelling power Γ^2 when the output frequency of the inverter has fluctuation where the inductance L_m is 115 nH and the capacitance C_m is 1.15 nF. Note that the LPF is designed in respects to the output impedance of $50+j0\ \Omega$ at 13.56 MHz. Assuming the frequency fluctuation of the inverter is ±1 MHz, the proportion of the reflected power to travelling power reaches up to 11.9%. It means that 11.0 % power loss occurs due to impedance mismatch. As a result, a standing wave occurs in the transmission line due to the reflected power. Therefore, the output impedance of the inverter has to be matched to the characteristic impedance of the inverter.

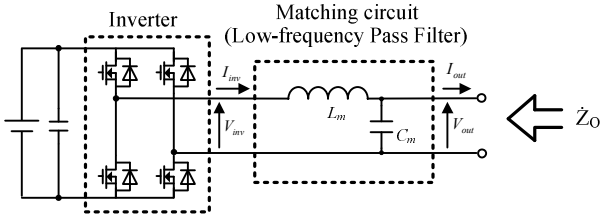

Figure 5. Basical matching circuit design without of consideration of the output frequency fluctuation.

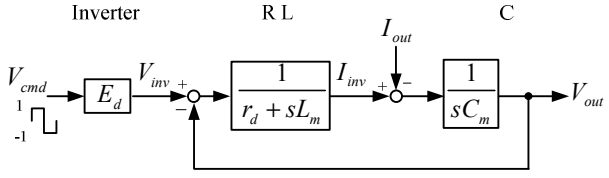

Figure 6. Block diagram of the power supply including the matching circuit.

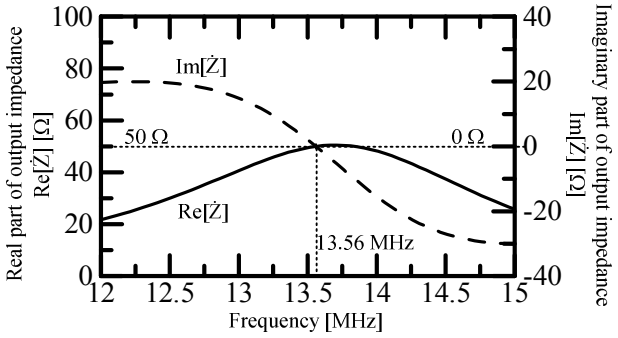

Figure 7. Frequency characteristic of output impedance.

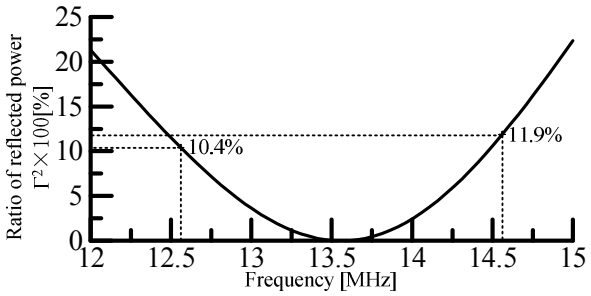

Figure 8. Frequency characteristic of reflected power.

V. SWITCHED-MODE MATCHING CIRCUIT TOPLOGY

Fig. 9 presents the proposed Switched-mode Matching Circuit (SMC). The SMC, which consists of six MOSFETs, two capacitors and two inductors, are connected to the output terminal of the inverter in series. As a result, the SMC shows the similar characteristics to the LPF. The switching frequency of the SMC is constrained by the output frequency of the inverter.

The specifications of the SMC are obtained by Table II. The switches of the $S_{1\text{-}4}$ are operated to make a variation of the output impedance of the inverter. The additional capacitance C_2 is connected to the L_1 in series when both the S_2 and S_3 or both the S_1 and S_4 are turn-on. On the other hand, the additional inductance L_2 is connected to the C_1 in parallel when both the S_3 and S_5 or both the S_4 and S_6 are turn-on. The SMC controls the timing of the switches. Therefore, the impedance of parallel connected L_2 and C_1 have same impedance to the C_m in Fig. 5. Additionally, the relationship between the L_1 and C_2 should respects to (13) when the output frequency has a fluctuation to f' [13]. Also, the output impedance should be matched to $\dot{Z}_O$ when the $S_{1\text{-}4}$ are turn-on. So, the inductor is designed to L_1=L_m and matches the output impedance.

$$2\pi f' L_1 > \frac{1}{2\pi f' C_2} \tag{13}$$

Fig. 10 shows the control brock diagram of the SMC. The two control methods are proposed in this paper. In both proposed control diagram, the switches of the matching circuit are synchronized with the output voltage of the inverter which is operated in square wave operation. The SMC is operated according to the frequency command f_{cmd}, duty D_m and phase command θ for $S_{1\text{-}4}$. The frequency command is decided based upon to the high transmission efficiency of the MRC. Note that, frequency tracking method is not discussed in this paper.

The gate signal is generated using a carrier comparison method. The carrier signal is provided to the comparator through the phase shifters which are controlled according to the phase command. The D_m controls the conduction time in each output period of the SMC which is equaled to the switching period because the domain of the D_m is from 0.5 to 1. Besides, two control block diagrams are considered. In the control diagram which shown in (a), the phase command which is used in the carrier comparison for $S_{1\text{-}4}$ is controlled. On the other hand, the phase command which is used for S_5 and S_6 is manipulated in control block diagram which shown in (b). The control periods of the D_m and θ are allowed to longer than the switching period of the inverter and SMC. The variation of the resonance frequency occurs as a result of the position gap between the transmitting coil and the receiving coil, is not changing rapidly.

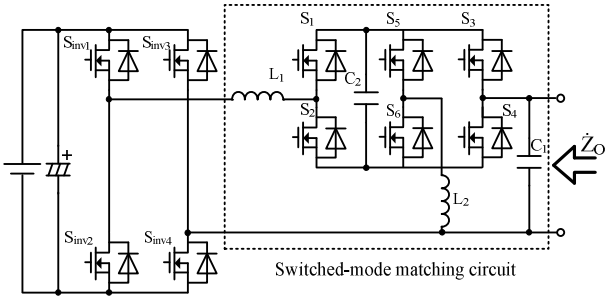

Figure 9. Switched-mode Matching Circuit (SMC).

TABLE II. SPECIFICATION OF SMC.

Items		Manufacturers	Value	
			1 MHz	13.56 MHz
MOSFET	$S_{inv1\text{-}4}$	Microsemi	ARF463BP1G (500V, 9A)	
	$S_{1\text{-}6}$			
Capacitor	L_1	TDK	1.5μH	114nH
	L_2	TDK	0.80μH	100nH
Inductor	C_1	TDK	47nF	2.5nF
	C_2	TDK	22nF	1.4nF

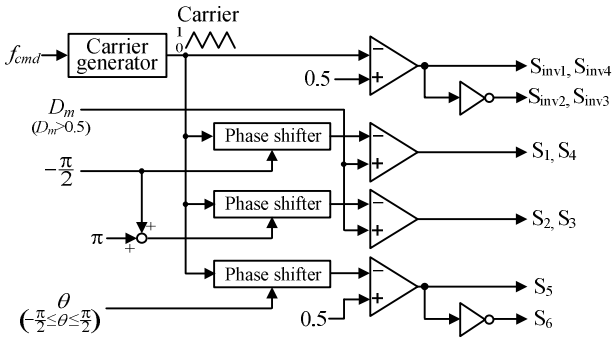

(a) Control method I.

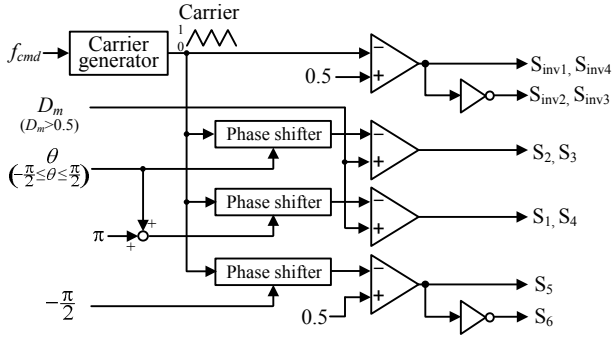

(b) Control method II.

Figure 10. Control block diagram of the SMC.

VI. Experimental Results

A. Experimental Methodology

In this chapter, the experimental results of the SMC are presented. Then experimental setup of the SMC including a square wave operated inverter and the carrier signal is provided from the FG. Note that, the output frequency and switching frequency are 1 MHz due the setup limitation. Then the parameters of the SMC are changed to L_1=1.5μH, L_2=0.75μH, C_1=47nF, C_2=22nF according to Table II.

i. On-off method for detection of output impedance

The on-off method is implemented to detect the output impedance of the inverter for experiments which is described later. The on-off method detects the output impedance of the inverter using the difference between the no-load output voltage and loaded output voltage. The output impedance is obtained by

$$\dot{Z}_o = \frac{\dot{V}_o}{\dot{I}} - R_{Load} \tag{14}$$

where $\dot{I}$ is the load current, R_{Load} is the load resistance and V_o is the source voltage which equals to no-loaded output voltage. When the load resistance does not include the imaginary part of the impedance, the load current is obtained by output voltage of the SMC and a phase difference between the output voltage of the inverter and output voltage of the SMC in terms of the fundamental components.

ii. Current injection method for detection of output impedance

The accuracy of the output impedance with the on-off method is lower than the current injection method. Therefore, the current injection method is used in generally as a detection method of the output impedance. The current injection method measures the voltage of the output terminal and current which is injected into output terminal. The injected current is a sinusoidal wave consists of the same frequency to the output frequency of the inverter. The output impedance is calculated by the amplitude and the phase between the generated voltage and injected current. Note that, when the output terminal voltage has distortion and DC bias, the detection of the phase returns an error. Thus, in such a way as to reject the DC bias and distortion, a Band-frequency Pass Filter (BPF) is added to the detector of the voltage and currents.

The on-off method as described previously is used in the experimental described in next chapter because the output impedance can be calculated simply compared to the current injection method. On the other hand, the current injection method is used in the simulation results to considerate the operation of the SMC in detail.

B. Experimental Waveforms of SMC with Control Block Diagram I

Fig. 11 shows the experimental results of the SMC and high frequency inverter with the control block diagram I when the duty D_m is 0.5 and phase command θ is 0˚. In these results, the switching frequency is approximately 1 MHz and the output voltage shows a sinusoidal waveform. During the no-load condition, the output voltage is 18.6 V_{rms}. On the other hand, output voltage of 14.2 V_{rms} is obtained when the resistance load 50 Ω is connected. In consequence, the output impedance 59.6 Ω is calculated using (14). In these conditions, the capacitor voltage of C_2 has resonance. Note that the calculated impedance has a margin of error due to a detection error of the phase angle between the drain-source voltage and output voltage. Besides, the output voltage of the inverter and output voltage waveform include the distortions due to the dead time. The distortions affect the accuracy.

Fig. 12 shows the experimental waveforms when the control parameters are changed to θ=-90˚. In these cases, the output voltage is 15.4 V_{rms} at no-load condition and 11.9 V_{rms} with resistance load of 50 Ω, respectively. Similarly, the output impedance 64.7 Ω is calculated using (14). In this case, the output impedance increases compared to condition of θ=0˚ because the voltage fluctuation of C_1 decreases. Therefore, the validity of the SMC can be confirmed. Also, to control the phase reference θ and duty D_m of the SMC, the output impedance of the inverter can be changed by using the SMC. It means that, the SMC can reduce the reflected power which occurs at the boundary point of the impedance due to the impedance mismatch to adopt the frequency tracking control.

C. *Simulation Results of SMC with Control Block Diagram II*

Fig. 13 shows the simulation results, where the output impedance is varied when the operating frequency is a constant value. The SMC is modeled using a circuit simulator to clarify the fluctuation of the output impedance. Note that the control block diagram II is used in this consideration. The matching circuit is designed to match the output impedance to 50+*j*0 Ω at D_m=1 and f_{cmd}=13.56 MHz. The simulation results yields that real part of the output impedance increase shown in (a) with changing the phase angle of carrier θ. The simulation results present that the phase command θ enables to control the real part of the output impedance. The phase command is controlled in the domain of between -90˚ and 45˚. Also both the real part and imaginary parts have fluctuations with increasing D_m. The detail of the operation will be considered.

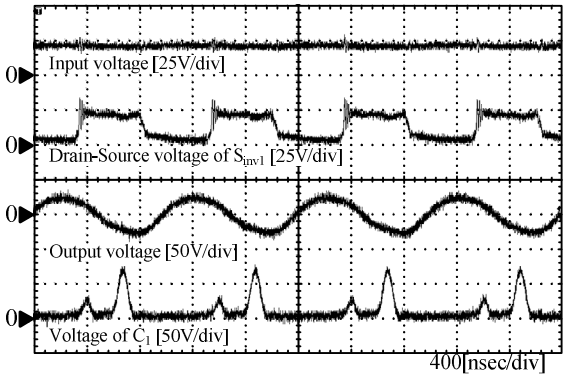

(a) No-load.

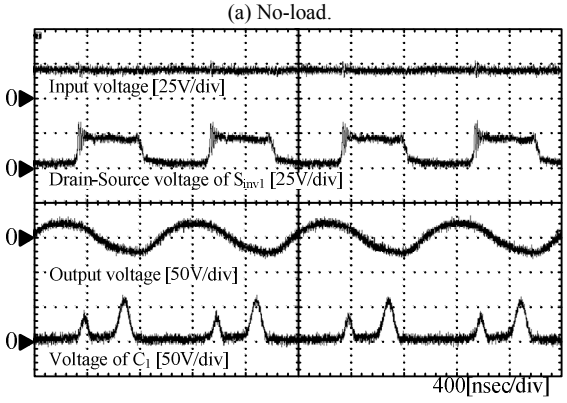

(b) 50 Ω load.

Figure 11. Experimental result of the SMC when the D_m=0.5, θ=0.

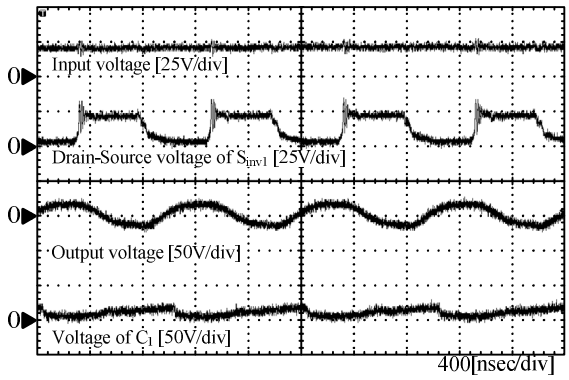

(a) No-load.

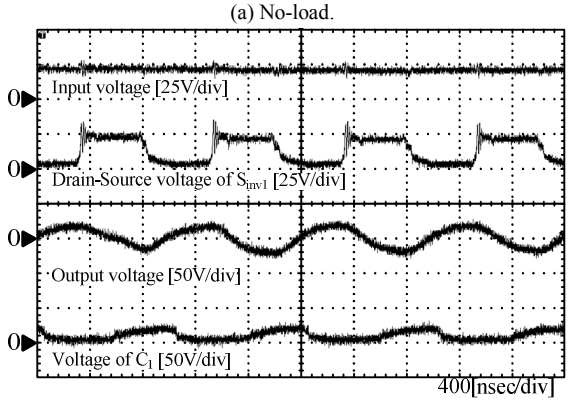

(b) 50 Ω load.

Figure 12. Experimental result of the SMC when the D_m=0.5, θ=-90˚

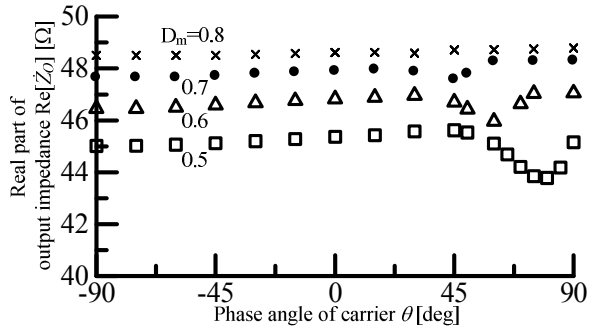

(a) Real part.

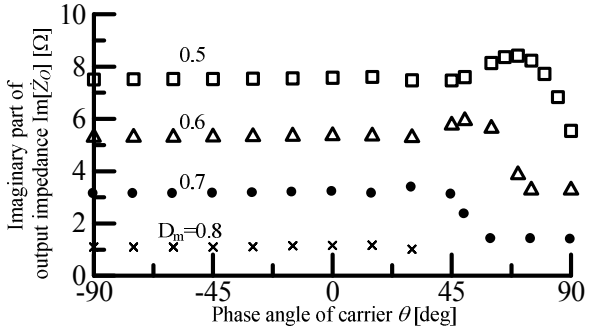

(b) Imaginary part.

Figure 13. Output impedance of the inverter including the SMC at constant frequency.

VII. CONCLUSION

In this paper, the matching circuit in the high frequency power supply for wireless power transfer with MRC is discussed. In the MRC system, the resonance frequency uses to obtain the maximum transmission efficiency has fluctuation is because of the transmission distance. Thus, the output frequency of the inverter needs to track the resonance frequency. In addition, the reflected power occurs at the high frequency region due to the impedance mismatch between the output impedance of the inverter and characteristic impedance of the transmission line. Therefore the output impedance of the high frequency power supply is required to match with the characteristic impedance of the transmission line despites of the output frequency. However, the fluctuation of the output frequency at the power supply affects the output impedance when the matching circuit is constructed by only inductor and capacitor. In this paper, the SMC which is used to adjust the output impedance of the power supply is proposed.

The experimental results confirmed that the output impedance has changed from 59.6 Ω to 64.7 Ω from the changes of the control parameter θ. In addition, the simulation results showed the control range of the SMC. Therefore, the simulation and experimental results also confirmed that the SMC can adjust the output impedance.

In the future work, the detail of the design method of the SMC will be optimized.

REFERENCES

[1] Z. N. Low, R. A. Chinga, R. Tseng, J. Lin, "Design and Test of a High-Power High-Efficiency Loosely Coupled Planar Wireless Power Transfer System," *IEEE Trans. On Industrial Electronics*, Vol. 56, No.5, pp. 1802-1812, 2009

[2] T. Ishiyama, "Non-contact power transmission technology for Communication Equipments," *Annual Conference of IEE of Japan Industry Applications Society (IEEJ JIASC)*, 1-S15-3-I, pp. 125-126, 2010 (in Japanese)

[3] A. Kurs, A. Karalis, R. Moffatt, J. D. Joannopoulos, P. Fisher, M. Soljacic, "Wireless Power Transfer via Strongly Coupled Magnetic Resonances," *Science*, Vol. 317, No. 5834, pp. 83-86, 2007

[4] A. Karalis, J. D. Joannopoulos, M. Soljacic, "Efficient Wireless non-radiative mid-range energy transfer," *Annals of Physics*, Vol. 323, No. 1, pp. 34-48, 2008

[5] B. L. Cannon, J. F. Hoburg, D. D. Stancil, S. C. Goldstein, "Magnetic Resonant Coupling As a Potential Means for Wireless Power Transfer to Multiple Small Receivers," *Power Electronics, IEEE Transactions on* , Vol. 24, No. 7, pp. 1819-1825, 2009

[6] J. O. Mur-Miranda, G. Fanti, F. Yifei, K. Omanakuttan, R. Ongie, A. Setjoadi, N. Sharpe, "Wireless power transfer using weakly coupled magnetostatic resonators," *IEEE Energy Conversion Congress and Exposition (ECCE)*, pp. 4179-4186, 2010

[7] S. Lee, R. D. Lorenz, "Development and validation of model for 95% efficiency, 220 W wireless power transfer over a 30cm air-gap," *IEEE Energy Conversion Congress and Exposition (ECCE)*, No. pp. 885-892, 2010

[8] K. Kusaka, S. Miyawaki, J. Itoh, "A Experimental Evaluation of a SiC Schotky Barrier Rectifier with a Magnetic Resonant Coupling for Contactless Power Transmission as a Power Supply", *Annual Conference of IEE of Japan Industry Applications Society (IEEJ JIASC)*, 1-41-I, pp.323-326, 2010 (in Japanese)

[9] T. Imura, H. Okabe, Y. Hori, "Basic experimental study on helical antennas of wireless power transfer for Electric Vehicles by using magnetic resonant couplings," *IEEE Vehicle Power and Propulsion Conference (VPPC)* , pp. 936-940, 2009

[10] T. Imura, H. Okabe, T. Uchida, Y. Hori, "Study on open and short end helical antennas with capacitor in series of wireless power transfer using magnetic resonant couplings," *Industrial Electronics (IECON)*, pp. 3848-3853, 2009

[11] Y. Ito, H. Akagi, Z. Yang, "Consideration from Viewpoint of Output Impedance Concerning Control Method for Parallel Operation of CVCF Inverters," *IEE of Japan Trans. D*, Vol.128, No.2,, pp.102-109, 2008 (in Japanese)

[12] K. Kusaka, J. Itoh, "A Fundamental Evaluation of a Power Supply of a Contactless Power Transmission with a Magnetic Resonant Coupling," *Annual Conference of IEE of Japan Industry Applications Society*, 1-108-I, pp. 507-510, 2011 (in Japanese)

[13] T. Takaku, T. Isobe, J. Narushima, H. Tsutsui, R. Shimada, "Power Factor Correction Using Magnetic Energy Recovery Current Switches," *IEE of Japan Trans. D*, Vol. 125, No. 4, pp. 372-377, 2005 (in Japanese)